Int. J. Heat Mass Transfer. Vol. 36, No. 16, pp. 3897–3907, 1993
Printed in Great Britain

0017–9310/93 $6.00+0.00

Study of 3-D mixing of a cold jet with a transverse plasma stream

ZOUHIR NJAH,† JAVAD MOSTAGHIMI,‡ M. FAGHRI§ and MAHER BOULOS†

† Plasma Technology Research Centre (CRTP), University of Sherbrooke, Sherbrooke, Québec, Canada, J1K 2R1

‡ Department of Mechanical Engineering, University of Toronto, Toronto, Ontario, Canada, M5S 1A5

§ Department of Mechanical Engineering and Applied Mechanics, University of Rhode Island, RI 02881, U.S.A.

(*Received* 8 *December* 1992 *and in final form* 4 *May* 1993)

Abstract—The present study involves both experimental and mathematical modelling of the 3-D mixing of a single jet with a transverse main stream. In the first part of this study, the interaction between a laminar nitrogen jet and a cross-flowing argon stream is studied under isothermal flow conditions. Results show that the numerical predictions of the nitrogen concentration fields, downstream of the injection point, are in good agreement with the experimental measurements. In the second part of this study, calculations of the mixing pattern between a single cold jet and a transverse plasma stream are presented. Results reveal a much slower gas mixing process under plasma conditions due to the increasing viscosity of the main stream. It is also shown that the mixing characteristics depend strongly on the ratio of jet to main stream mass fluxes ($R_m = \rho_i v_i / \rho_0 w_0$).

1. INTRODUCTION

THE QUESTION of mixing of a cold jet introduced in a thermal plasma reactor is of great interest in plasma chemistry applications. A successful plasma chemical process depends to a large extent on the knowledge of the velocity, temperature and concentration fields in the region where the reactants are injected. Plasma flows are characterized by their high temperature and the presence of steep temperature gradients. As the viscosity of gases increases with temperature, the flow pattern in the mixing zone of a cold jet with a plasma stream is significantly different from that for an isothermal flow at ambient temperature; a substantial reduction of the mixing between the two streams under plasma conditions is observed despite the increased mass transfer coefficient in the high temperature region. This fact has been clearly demonstrated by Dundas [1] who reported concentration mapping for an argon/air system under isothermal ambient temperature and plasma conditions.

In a plasma reactor the side jet could be either one of the reactants or a quench medium introduced to rapidly cool a reaction mixture and thus avoid product decomposition. It may be noted that in radio frequency (r.f.) plasma reactors, two techniques are commonly used to inject reactants into the plasma; these are either introduced by a side jet downstream of the coil region of the discharge, or through a central water cooled probe. Extensive reviews of the subject has been published by Akashi [2], Yoshida [3] and Boulos [4].

Because of the practical importance of jets discharging into transverse streams, a large number of experimental, analytical and computational investigations have been carried out on this subject. Experimental investigations of the behavior of jets issuing normally into a cross stream have been mostly devoted to measuring the jet trajectory, jet spread, velocity, temperature and pressure fields. Jordison [5] was the first to determine experimentally the trajectory of a jet issuing perpendicularly into a cross flow. He defined the trajectory of the jet as the line joining the points of maximum velocity. Keffer and Baines [6], Keffer [7], and Platten and Keffer [8] studied the general features of a jet injected normally into a cross stream and presented data for the jet trajectory. A comprehensive physical description of the jet in a cross stream is given by Moussa *et al.* [9]. Patrick [10] reported velocity and concentration measurements for the mixing of a round turbulent jet with a transverse main stream. His results showed that the flow pattern is dominated by a pair of vortices attached to the jet, which promote rapid mixing. Gelb and Martin [11], Wu *et al.* [12], and McMahon and Mosher [13] made measurements of the pressure fields resulting from the interaction of a jet with a cross stream. Margason [14], McMahon *et al.* [15] and Mikolowsky and McMahon [16] studied the jet–wake interference effects associated with jets exhausting into a deflecting stream. Ramsey [17], and Ramsey and Goldstein [18] studied the interaction between a single heated jet and a cross stream and reported measurements of velocity, temperature, and turbulence fields. Campbell and Schetz [19] investigated the behavior of heated jets discharged into waterway and determined the growth of the jet for different discharge velocities and temperatures. Kamotani and Greber [20] reported measurements of the velocity, temperature, and turbulence intensity fields for single, multiple, opposing

NOMENCLATURE

c	nitrogen mass fraction
c_p	specific heat at constant pressure
C_s	speed of sound
D	binary diffusion coefficient
h	enthalpy
k	thermal conductivity
p	pressure
Pe	Peclet number
Pr	Prandtl number
R	ideal gas constant; also stands for the reactor radius
Re	Reynolds number
R_m	ratio of jet to main stream mass fluxes, $\rho_i v_i/\rho_0 w_0$
T	temperature
$\vec{u}$	velocity vector, (u, v, w)
u, v, w	velocity components in x, y, z directions
x, y, z	Cartesian coordinates
z^*	distance from the injection point, $z - z_i$.

Greek symbols

γ	ratio of heat capacities, c_p/c_v
Γ	artificial (false) viscosity
μ	dynamic viscosity
ν	cinematic viscosity
ρ	density
$\bar{\bar{\tau}}$	viscous shear stress.

Subscripts

0	main stream gas
f	false
i	injected gas
s	sound
w	solid wall.

and plane jets. Special attention was given to the structure of the rotational velocity field which results because of the shearing action between the main stream flow and the edge of the jet. In the experiments of Rudinger [21], the principal aim was to measure the penetration of side jets introduced in a cross flowing stream through a narrow slot. Chassing *et al.* [22] made measurements of the flow characteristics of coaxial jets as well as on a single jet in the presence of a cross stream. Bergeles *et al.* [23] studied the flow field created by the injection of a circular air jet normal to a plane past which an external stream is flowing. Particular attention has been given to obtain details on the flow field in and around the point of injection of a single jet in a cross stream. Crabb *et al.* [24] used laser doppler anemometry to measure the velocity in the near field of a round jet normal to a cross flow. Rajaratnam and Gangadharaiah [25] conducted an experimental study on the entrainment characteristics of circular jets in cross flows and suggested a correlation for the entrainment coefficient. In a series of publications, Andrepoulos [26–28] reported detailed measurements of wall static pressure, velocity and temperature fields associated with a jet in a cross flow. He also studied the structure of the deflected jet by spectral analysis and flow visualization for various jet to main stream velocity ratios. More recently, Sherif and Pletcher [29–31] concentrated their efforts on studying the thermal characteristics of heated turbulent jets injected into a transverse stream and presented measurements of the flow, thermal and turbulence characteristics in the interaction zone with special attention to the jet-wake region.

Analytical studies devoted to the mixing pattern between jets and cross-flowing streams are not as numerous as experimental investigations. Platten and Keffer [32] suggested, in their analytical model, that the jet deflection is due to the entrainment of the cross flow in the jet. By allowing the entrainment coefficient to vary with velocity ratio and jet deflection angle, they obtained good agreement with test data. Ziegler and Wooler [33] developed an analytical model based on the solution of the continuity and momentum equations for the jet trajectory. Good agreement between theory and available experimental data were obtained for the surface pressure distributions. Kim [34] based his analytical approach on jet trajectory, jet diffusion layer, and flow establishment to predict the mixing characteristics of a cold jet injected at an angle into a hot cross flow. Karagozian [35] suggested an analytical model for the vorticity associated with a transverse turbulent jet. Particular emphasis was placed on the vortex pair associated with the jet.

Computational work on the interaction between jets and cross flows is somewhat limited. Chien and Schetz [36] used a vorticity–velocity method to obtain numerical solutions for an unheated and buoyant jet in a cross flow. Patankar *et al.* [37] used a finite-difference procedure to predict the flow field resulting from the interaction of a round jet and a main stream. The predictions were in satisfactory agreement with experimental data for the jet trajectory. Bergeles *et al.* [38] employed a three-dimensional finite-difference procedure similar in many respects to that used by Patankar *et al.* [37] to the analysis of the flow and thermal fields created by a jet exhausting into a cross flowing stream. The results obtained were in good agreement with the measured behavior only for jet to cross flow velocity ratios less than 0.1. Demuren [39] compared two three-dimensional finite-difference procedures to predict the flow field of a row of jets issuing normally into a cross stream. He found that the hybrid

central/upwind scheme used in representing the convection term is superior to the upstream weighed difference scheme. More recently, Lana and Viollet [40] presented a three-dimensional treatment of the mixing of a plasma jet into a cold flow.

The present paper presents the results of a three-dimensional laminar model used for the prediction of the mixing of a single jet issuing normal to a main stream. Results are presented in two parts. The first is devoted to a study of an isothermal system for which experimental concentration measurements were used for the validation of the model predictions. In the second part, numerical predictions of the mixing of a lateral round jet introduced in a plasma cross stream are reported. Special attention is given to obtain details of the temperature and concentration fields downstream of the injection point.

2. MATHEMATICAL FORMULATION AND NUMERICAL PROCEDURE

A schematic of the studied system is given in Fig. 1. It is composed of a 50 mm i.d. cylindrical tube, 250 mm long. The lateral gas jet is introduced, 50 mm downstream the entrance section of the main stream, from a 4 mm i.d. orifice.

2.1. *Basic assumptions*

The mathematical model developed in this study is based on the following assumptions.

(1) Steady, laminar and incompressible fluid flow.
(2) 3-D Cartesian (x, y, z) system of coordinates.
(3) Binary flow, heat and mass transfer.
(4) Viscous dissipation is neglected.
(5) Gravity effects are neglected.

2.2. *Governing equations*

Following the prescribed assumptions, the continuity, momentum, energy and concentration equations can be written in vector notation as follows:

continuity equation:

$$\vec{\nabla}\cdot(\rho\vec{u}) = 0 \tag{1}$$

momentum equations:

$$\rho\vec{u}\cdot(\vec{\nabla}\vec{u}) = -\vec{\nabla}p - \vec{\nabla}\cdot\bar{\bar{\tau}} \tag{2}$$

energy equation:

$$\rho\vec{u}\cdot(\vec{\nabla}h) = \vec{\nabla}\cdot\left(\frac{k}{c_p}\vec{\nabla}h\right) \tag{3}$$

concentration equation:

$$\rho\vec{u}\cdot(\vec{\nabla}c) = \vec{\nabla}\cdot(\rho D\vec{\nabla}c) \tag{4}$$

where $\vec{u}: (u, v, w)$ is the velocity vector, ρ is the density, $\bar{\bar{\tau}}$ is the viscous shear stress tensor, p is the pressure, h is the enthalpy, k is the thermal conductivity, c_p is the specific heat at constant pressure, c is the concentration (mass fraction) of the injected gas and D is the binary diffusion coefficient.

The thermodynamic and transport properties for argon and nitrogen were obtained as functions of temperature from ref. [41]. Mixture rules [42] were employed for the calculation of the thermodynamic and transport properties as functions of composition; the density of a mixture of gases A and B is obtained, for example, as follows:

$$\rho = c\rho_A + (1-c)\rho_B \tag{5}$$

where ρ is the density of the mixture, c is the mass fraction of A in the mixture, ρ_A and ρ_B are respectively the density of A and B gases under the local mixing conditions.

2.3. *Boundary conditions*

The boundary conditions are presented for the numerical treatment of the mixing of single round jet with a cross stream (Fig. 1). In this case, equations (1)–(4) are subject to the following boundary conditions:

- Entrance of the main stream

At the entrance section, the main stream was assumed to have a uniform temperature (T_0) and velocity (w_0) profiles.

$$T = T_0, \quad w = w_0, \quad u = v = 0, \quad c = 0.$$

- Entrance of the jet

At the origin, the jet was assumed to have a uniform temperature (T_i) and velocity (v_i) profiles.

$$T = T_i, \quad v = v_i, \quad u = w = 0, \quad c = 1.$$

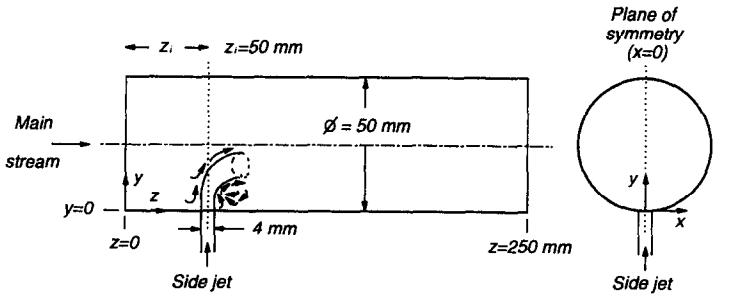

FIG. 1. Schematic of the studied system.

• Plane of symmetry

The yz plane through the origin of the jet is treated as a plane of symmetry.

$$u = \frac{\partial v}{\partial x} = \frac{\partial w}{\partial x} = \frac{\partial h}{\partial x} = \frac{\partial c}{\partial x} = 0.$$

• Solid wall

$$T = T_w, \quad u = v = w = 0, \quad \frac{\partial c}{\partial x} = \frac{\partial c}{\partial y} = 0.$$

• Exit plane

At the exit, the boundary conditions are not known. However, if the exit Peclet number ($Pe = Re \cdot Pr$) is sufficiently large, one can safely assume that the axial derivatives of the velocity, temperature and concentration are equal to zero.

$$\frac{\partial u}{\partial z} = \frac{\partial v}{\partial z} = \frac{\partial(\rho w)}{\partial z} = \frac{\partial h}{\partial z} = \frac{\partial c}{\partial z} = 0.$$

2.4. *Solution procedure*

The solution procedure is based on the SIMPLE algorithm (Semi-Implicit Method for Pressure Linked Equations) developed by Patankar and Spalding [43] and described in ref. [44] for three-dimensional elliptic situations. Only the important features of the procedure are described here. The governing equations are written in terms of the primitive variables, i.e. velocities, pressure, enthalpy, and concentration. The finite-difference equations are obtained by integrating the differential equations over a control volume surrounding each grid point and expressing the variation of variables in each direction by suitable profile approximations. The combined effect of convection and diffusion is handled by a power law scheme described in ref. [44]. Finite-difference equations are solved by a line by line method.

To overcome the difficulty associated with the determination of the pressure field, the continuity equation is converted into a pressure correction equation. From a guess of the pressure field, the momentum equations are solved to obtain the preliminary velocity field, which in general, does not satisfy the continuity equation. Appropriate corrections to the pressure field are computed from the pressure correction equation. The velocities are then corrected using velocity-correction formulas. We notice that the coefficient in the finite-difference equations depend on the variables themselves. Thus, computations proceed by iterations with the coefficients continuously updated from one iteration to the next.

Calculations were carried out with a non-uniform grid spacing, the grid points were arranged so that they are densely packed close to the injection point where the gradients are the highest. For regions away from the injection point the grid spacing is gradually increased. Convergence was reached when, from one iteration to the next, the value of each of the dependant variables changed by less than 0.001% of the maximum value of its field. Using $20 \times 32 \times 60$ grid nodes in the x, y and z directions respectively, 2000 iterations were generally required in order to reach a converged solution. Each such iteration needs about 40 s on an IBM RISC 530/6000 computer.

Preliminary tests were performed to explore the grid dependency of the numerical results. The grids in each direction were refined until negligible differences (less than 1%) were found between predictions of the two finer spacing. A grid with $20 \times 32 \times 60$ nodes in the x, y and z directions, respectively, was sufficient to insure our numerical solutions to be grid-independent for plasma and isothermal cases.

Since the computer program used in this study was written for a Cartesian grid, the cylindrical configuration of the duct for the main stream was approximated by rendering inactive 'blocking-off' the control volumes outside the flow domain. The blocking-off operation consists of establishing known values of the relevant dependant variables. In our case the inactive region is handled as a stationary solid. In other words the boundary conditions described for the solid wall stands for the inactive region.

The SIMPLE algorithm is usually used to solve incompressible flows with constant density. Although large variations of the density are observed in our system, the flow is indeed incompressible. Since the local Mach number is considerably smaller than unity, changes in density are in this case entirely due to the variations in the temperature, rather than pressure. It may be noted that the speed of sound, C_s, in an ideal gas is given by:

$$C_s = \sqrt{(\gamma RT)} \tag{6}$$

where $R = 207.8$ J kg^{-1} K^{-1}. For argon at atmospheric pressure and 5000 K, $\gamma = 5/3$ and $C_s \approx 1316$ m s^{-1}. If we consider that the maximum velocity in a r.f. plasma reactor is less than 100 m s^{-1}, the maximum Mach number will be less than 0.08. The incompressible nature of the flow is also confirmed by our results where the maximum pressure difference in our calculation domain is only a few percent of the total pressure.

On the question of artificial viscosity, we notice that according to Patankar [44], the artificial viscosity is given for a two-dimensional flow field by:

$$\Gamma_t = \frac{\rho U \Delta x \Delta y \sin 2\theta}{4(\Delta x \sin^3 \theta + \Delta y \cos^3 \theta)} \tag{7}$$

where U is the resultant velocity, θ is the angle between the velocity vector and the x-coordinate, Δx and Δy are the grid spacings. For $\theta = 0$, $\Gamma_t = 0$. The maximum artificial viscosity is observed for $\theta = 45°$:

$$\Gamma_{t,max} = \frac{\rho U \Delta x \Delta y}{\sqrt{(2)}(\Delta x + \Delta y)} \tag{8}$$

and the ratio between $\Gamma_{t,max}$ and molecular viscosity μ is given by:

$$\frac{\Gamma_{t,max}}{\mu} = \frac{U}{v}\left(\frac{\Delta x \Delta y}{\sqrt{(2)}(\Delta x + \Delta y)}\right) \tag{9}$$

for the case where $\Delta x = \Delta y$, equation (9) can be written as:

$$\frac{\Gamma_{f,max}}{\mu} \approx 0.35 \frac{U\Delta x}{\nu} \tag{10}$$

for $\Delta x = 0.5 \times 10^{-3}$, $\nu = 6 \times 10^{-3}$, $U = 10$ m s^{-1}, we obtain:

$$\frac{\Gamma_{f,max}}{\mu} \approx 0.29. \tag{11}$$

It is to be noted that an inspection of the flow field indicates that only a small number of grids are in such a situation. The vast majority of the control volumes in the flow are parallel to grid-lines giving rise to a negligible artificial viscosity.

3. EXPERIMENTAL SETUP

In order to calibrate the model against experimental data and to learn about its capabilities and limitations, an experimental study of the isothermal injection of a nitrogen jet into an atmospheric argon stream is conducted. A schematic of the experimental setup is given in Fig. 2. The measurements of nitrogen concentration (mass fraction) were performed in a 50 mm i.d. tube which was supplied with a nearly uniform-velocity stream of argon. The side jet was introduced a distance of 50 mm from the main stream inlet through a 4 mm i.d. port. The tube was carefully installed to provide a vertical symmetry plane and then limit the experimental investigation to half of the flow field. The gas sample was taken using a stainless steel probe (2.8 mm o.d., 1.8 mm i.d.) supported by an appropriate traversing mechanism controlled manually. The gas sample was transported through a stainless steel capillary tube, to the mass spectrometer (MS) for gas analysis. It may be noted that the capillary line was about 10 m long. In this condition the response time was determined to be approximately 15 s by exposing the probe to a pulse of the tracer gas (N_2) and measuring the time needed for the peak to be detected by the MS. A set of micrometric valves was used to control the gas flow rate in the capillary. The inlet pressure to the MS was maintained at 130 Pa (about 1 Torr).

The mass spectrometer used was a VG Micromass-PC 300 D, Quadrupole MS. It is essentially composed of an ion source, a mass filter and a collector. In the ion source, a thoriated iridium filament at 2 A produce the positive ions with an energy level of 70 eV. These ions are separated by the mass filter (Quadrupole) and collected in a standard Faraday cup. The vacuum in the MS is maintained at an absolute pressure of 10^{-3}–10^{-4} Pa by a turbomolecular pump backed by a 2 stage rotary mechanical pump. An IBM PC with appropriate software was used to control the operation of the MS.

For quantitative analysis, the detector was calibrated using a standard Ar/N_2 gas mixture containing 10% vol. N_2. Helium was used as a purge gas in order to measure the residual background level of these gases in the MS. Measurements of the N_2 concentration, at one tube diameter downstream of the injection point, on each side of the symmetry plane are found to be comparable within $\pm 1\%$. It may be noted that a full scan of the concentration profile on the plane of symmetry took 10 min. In these conditions it was necessary to insure that the system conditions did not vary during this period. Measurements of the gas composition at a fixed location were quite satisfactory in this respect as they revealed negligible composition fluctuations over a 10 min period. Finally we notice that our concentration measurements were reproducible within $\pm 2\%$.

4. RESULTS AND DISCUSSION

Results are presented in two parts. First, the isothermal injection of nitrogen into atmospheric argon is studied both numerically and experimentally. Next, a numerical study is conducted for the mixing of the side jet with a transverse argon plasma stream.

4.1. *Cold jet injection in a cold cross stream*

Two preliminary tests were performed, under isothermal flow conditions, for a nitrogen jet ($T_i = 300$

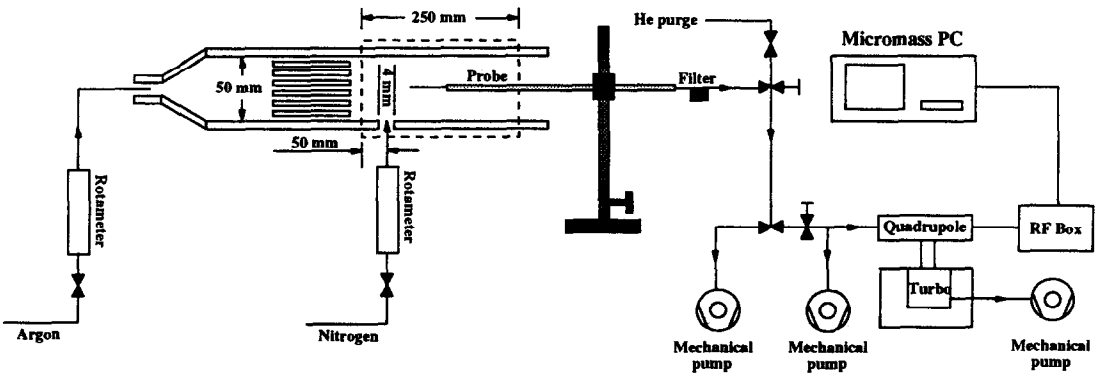

FIG. 2. Experimental setup.

K) discharging normally into a nearly uniform argon stream ($T_0 = 300$ K). The argon stream velocity was set equal to 0.5 m s^{-1} ($Re = 1862$) and the ratio of nitrogen to argon mass fluxes ($R_m = \rho_i v_i / \rho_0 w_0$) is fixed at 3.9 in the first case and at 7.8 in the second case. For $R_m = 3.9$, the experimental and computed nitrogen mass fraction profiles, on the plane of symmetry, at $z^* = z - z_i = 4, 8, 16$ and 32 mm downstream the injection point, are presented in Fig. 3. This figure shows that the predictions of the 3-D laminar model are in satisfactory agreement with the experimental measurements specifically around the jet trajectory which corresponds to the location of the maximum nitrogen mass fraction. We notice, however, that the model underestimates the jet diffusion near the wall. Figure 3 also shows that the spread of the jet is a strong function of the distance downstream of the injection point. Corresponding measured and computed nitrogen mass fraction profiles for $R_m = 7.8$ are given in Fig. 4. The agreement is also quite satisfactory though we notice that, at 4 mm downstream of the injection point, it is not as good as those obtained farther downstream. This may be attributed to the coarse orthogonal mesh and to the experimental difficulties for the proper sampling of the gases in this region without disturbing the flow. A comparison between nitrogen mass fraction profiles obtained at $z^* = 4$ mm with $R_m = 3.9$ (Fig. 3(a)) and $R_m = 7.8$ (Fig. 4(a)) shows that the increase of the jet velocity results in a deeper penetration of the side jet in the main stream and in a better mixing between the two gas streams. In other words, this comparison proves that the trajectory and spread of the jet depend strongly on the blowing parameter R_m.

4.2. *Cold jet injection in a cross plasma stream*

In this case, the results of a numerical study of the mixing of a side cold nitrogen jet ($T_i = 300$ K) with a transverse argon plasma stream ($T_0 = 8000$ K, $T_w = 400$ K) are presented. Before discussing the mix-

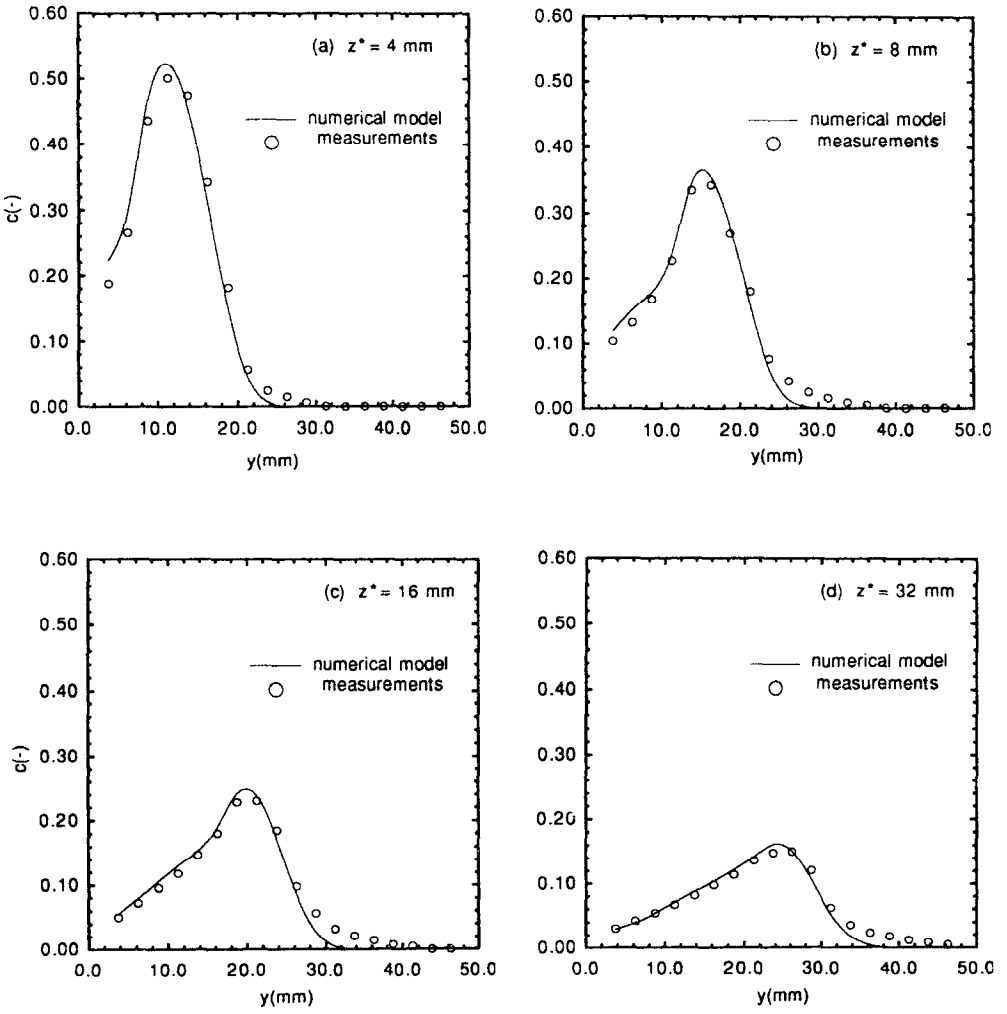

FIG. 3. Computed and measured nitrogen mass fraction profiles on the plane of symmetry ($R_m = 3.9$, $z^* = z - z_i$).

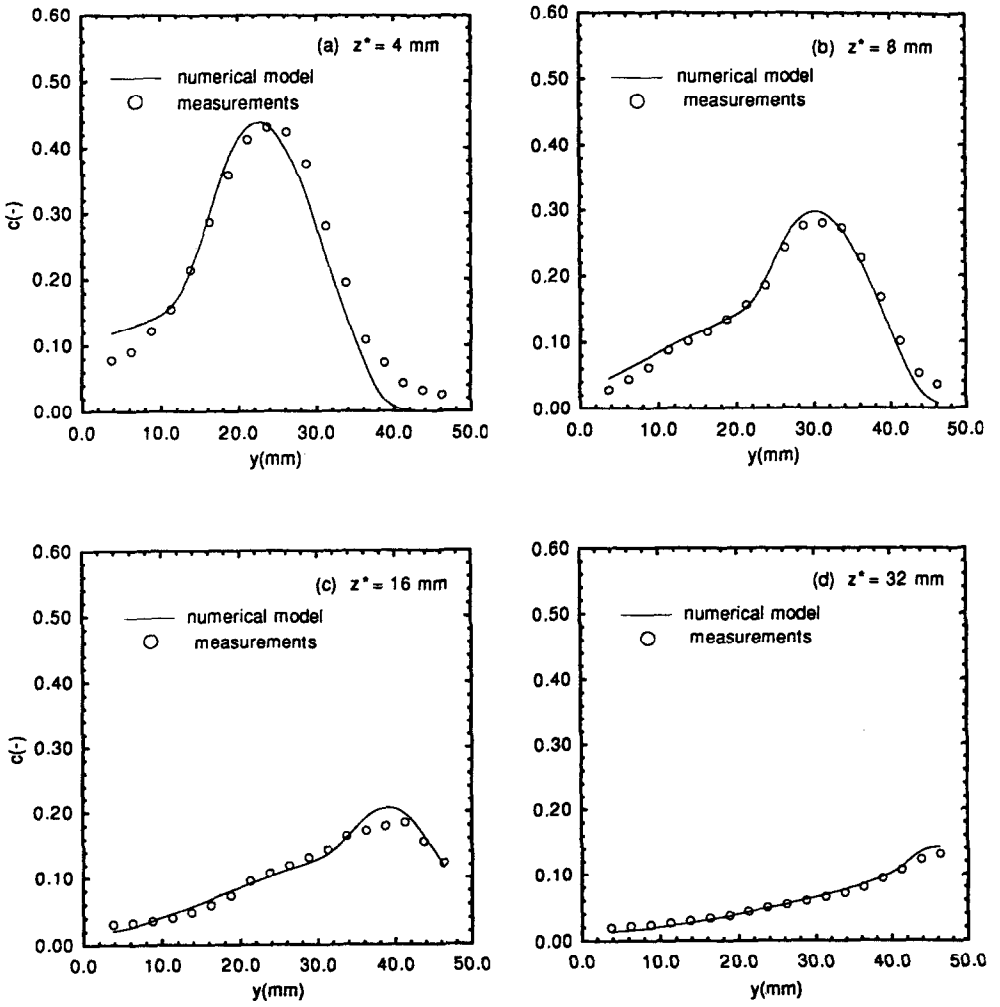

FIG. 4. Computed and measured nitrogen mass fraction profiles on the plane of symmetry ($R_m = 7.8$, $z^* = z - z_i$).

ing characteristics resulting from such an interaction, the effects of the temperature and gas composition on the viscosity (μ) and the mass diffusion coefficient (ρD) for Ar/N_2 mixtures are repored in Fig. 5. From Fig. 5(a) one can see that, in the range 300–13 000 K, the viscosity decreases slightly with increasing nitrogen concentration while Fig. 5(b) shows that the mass diffusion coefficient depends strongly on the composition for $T \geqslant 6000$ K. A higher concentration of nitrogen results in a smaller mass diffusion coefficient. Since D is independant of the mixture composition, the variation of ρ is mostly responsible for such variation of ρD.

Two flow conditions are considered here. In the first one the inlet argon plasma main stream velocity and temperature are set equal to 10 m s^{-1} and 8000 K, while the injected gas velocity and temperature are set at 2.52 m s^{-1} and 350 K ($R_m = 3.9$). In the second case the inlet velocity and temperature of the argon plasma flow are kept constant, while the side jet velocity is increased to 5.04 m s^{-1} ($R_m = 7.8$).

First, the velocity vector, temperature and concentration fields in the plane of symmetry are presented in Fig. 6 for $R_m = 3.9$. One can see from Fig. 6(a) that at the source, the jet trajectory is almost unaffected by the presence of the main stream. In this small region, the obstructing jet decelerates the plasma stream at its upstream surface giving rise to a region of positive pressure and becomes subject to intense shear stresses which eventually causes its deflection; the main stream forces the jet to deflect and a reverse flow region, called the wake-jet region, appears downstream of the injection point. This region of negative pressure is characterized by a pair of contra-rotating vortices, attached to the jet, which promote rapid mixing between the two streams. Figures 6(b) and (c) show, in the plane of symmetry, the temperature and the mass fraction of nitrogen distributions resulting from such an interaction. The reduced penetration of the jet is clearly noticeable under these flow conditions compared to that for a cold flow for same R_m ratio. Figure 6(b) indicates that the introduction of the cold

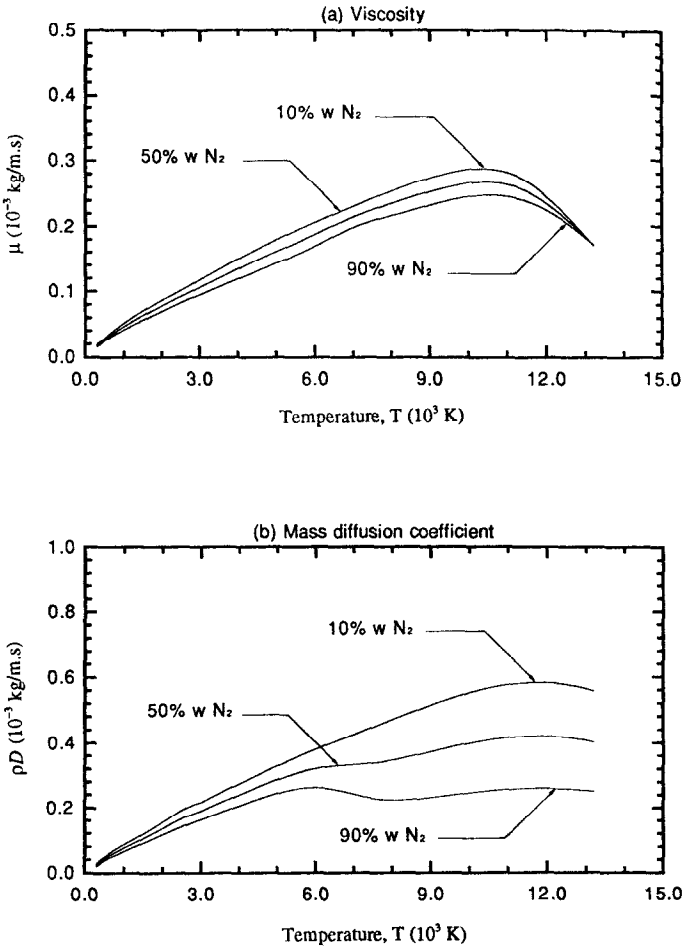

FIG. 5. Viscosity and mass diffusion coefficient of argon–nitrogen mixtures as functions of temperature.

jet causes a local and rapid cooling of the plasma flow. This figure also reveals interesting information on the flow character in the jet-wake region; for low injection velocities, the fluid temperature near the wall is significantly affected by the temperature of the jet fluid. This is in effect that which occurs in discrete film cooling, except that more than one jet is used, and the injection parameter R_m may be slightly lower for effective cooling processes. In the same order of ideas, the nitrogen mass fraction distribution presented in Fig. 6(c) shows the tendency to early reattachment of the injected gas to the wall. Since the jet is bent so sharply and its wake region is so narrow, one can conclude that convection does not play a major role in the mixing process and that molecular diffusion controls the essential characteristics of the mixing process in this case.

Next, the velocity vector, temperature and concentration distributions, in the plane of symmetry, are presented in Fig. 7 for $R_m = 7.8$. In this case all the operating conditions are the same as before except for the increase of the injection velocity from 2.52 to 5.04 m s^{-1}. A comparison between the velocity vector, temperature and concentration fields obtained with $R_m = 3.9$ (Fig. 6) and $R_m = 7.8$ (Fig. 7) shows that as the injected momentum flux increases, the injected gas penetrates more easily the main stream, spreads more quickly, and causes a more rapid cooling of the plasma flow. Examination of Figs. 6(b) and 7(b) indicates that for low injection velocities, the fluid temperature in the jet wake region is significantly affected by the temperature of the jet fluid while this is unlikely to happen for larger injection velocities. In Fig. 8 the mass nitrogen concentration profiles in the plane of symmetry are presented for three locations downstream of the injection point. This figure shows that with $R_m = 3.9$, molecular diffusion controls the essential features of the mixing process while with $R_m = 7.8$ convection plays a more important role in the mixing between the two gases. Finally, a comparison between the isothermal and plasma cases, of the maximum of nitrogen mass fraction at different locations downstream of the injection point is presented in Fig. 9. The results show that it is more difficult to achieve good mixing between the two streams under plasma conditions compared to that at room tem-

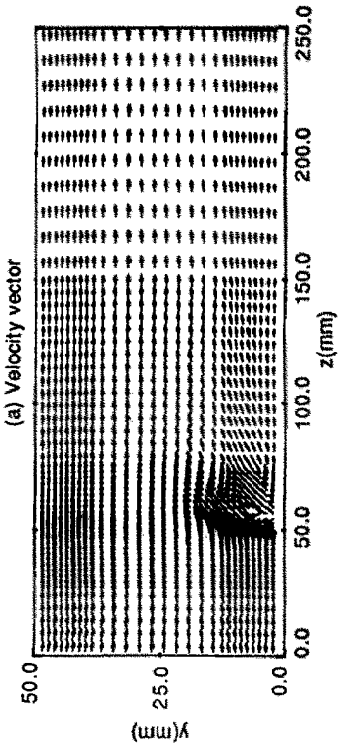

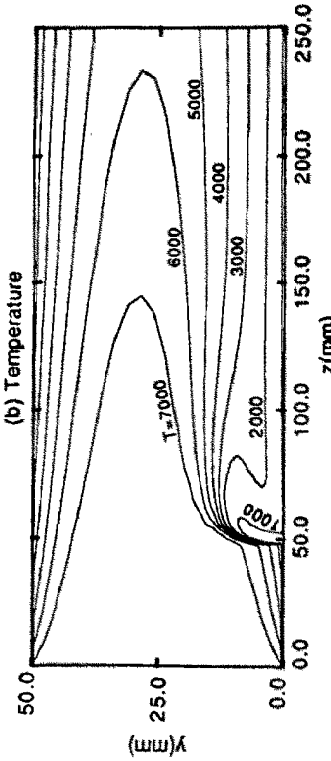

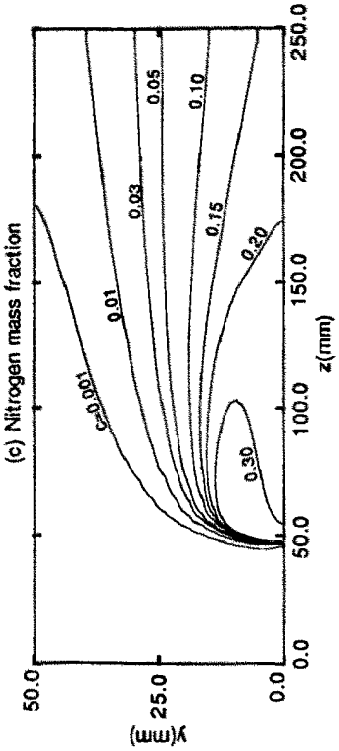

FIG. 7. Velocity vector, temperature and nitrogen mass fraction distributions on the plane of symmetry ($T_0 = 8000$ K, $T_i = 300$ K, $R_m = 7.8$).

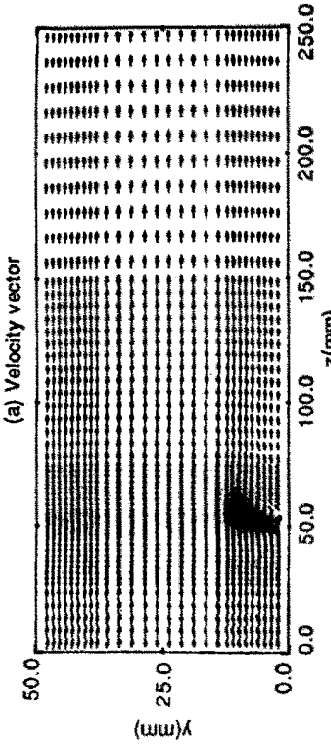

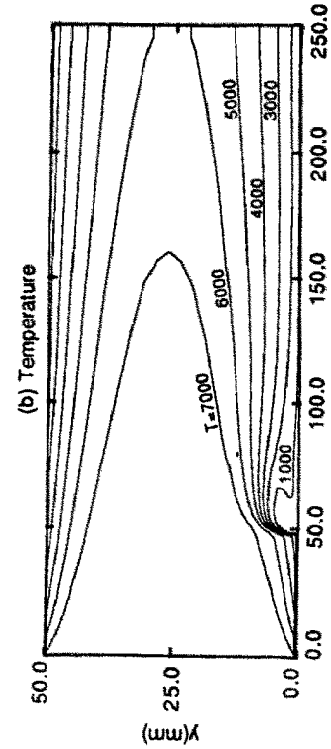

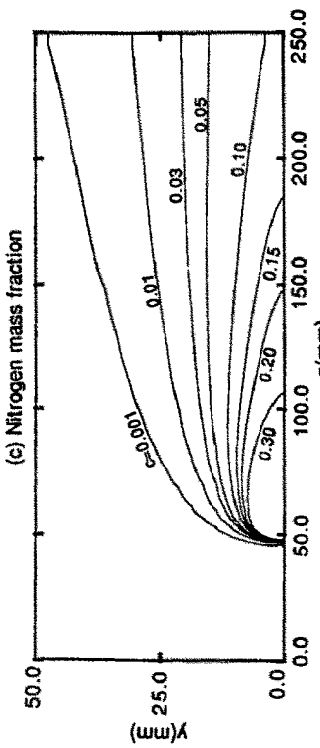

FIG. 6. Velocity vector, temperature and nitrogen mass fraction distributions on the plane of symmetry ($T_0 = 8000$ K, $T_i = 300$ K, $R_m = 3.9$).

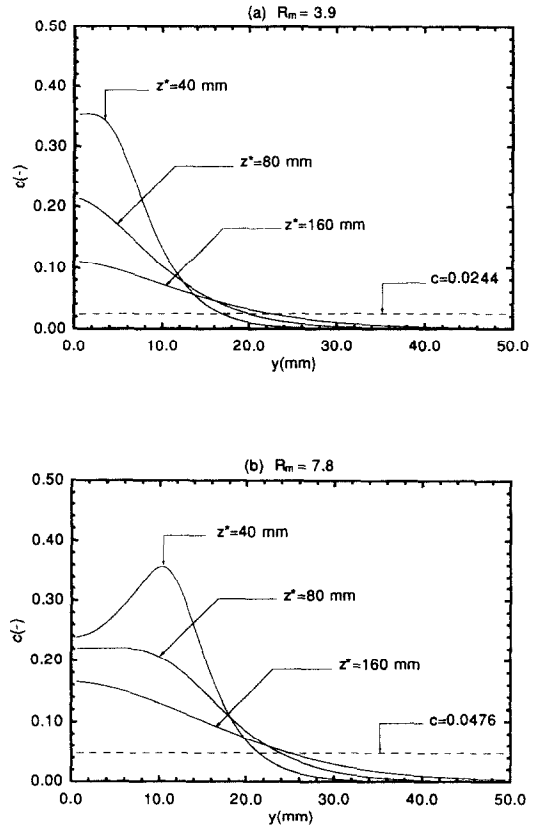

FIG. 8. Nitrogen mass fraction profiles on the plane of symmetry ($z^* = z - z_i$).

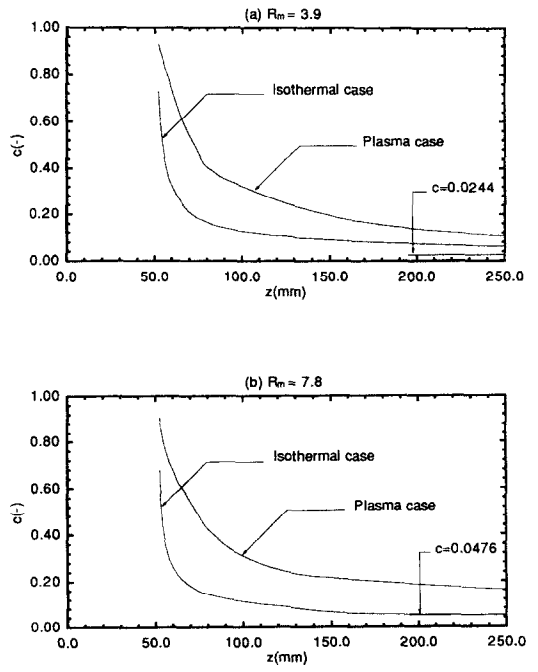

FIG. 9. Variation of the maximum nitrogen mass fraction downstream of the injection point.

perature. This is attributed to a lower ratio of jet to main stream momentum fluxes in the plasma case and to the high viscosity of the gases under plasma conditions. This figure also shows that an increase in the jet mass flux contributes to a better mixing.

5. CONCLUSION

The following conclusions may be drawn from this study:

- The predictions of the 3-D laminar model are in good agreement with the experimental measurements for the isothermal case.
- The temperature and concentation fields depend strongly on the ratio of jet to main stream mass fluxes.
- The gas mixing under plasma conditions is substantially more difficult compared to that at room temperature due essentially to the high viscosity of the plasma.

Acknowledgements—The financial support by the Natural Sciences and Engineering Research Council of Canada (NSERC) and by the Ministry of Education of the Province of Québec is gratefully acknowledged.

REFERENCES

1. P. H. Dundas, Induction plasma heating: measurements of gas concentrations, temperature and stagnation heads in a binary plasma system, NASA CR-1527 (1970).
2. K. Akashi, Progress in thermal deposition of alloys and ceramic fine particles, *Pure Appl. Chem.* **57**, 1197–1206 (1985).
3. T. Yoshida, The future of thermal plasma processing, *Mater. Trans. J. Jap. Inst. Metals* **31**, 1–11 (1990).
4. M. I. Boulos, Thermal plasma processing, *IEEE Trans. Plasma Sci.* **19**, 1078–1089 (1991).
5. R. Jordison, Flow in a jet directed normal to the wind, British Aeronautical Research Council, R & M 3074 (1956).
6. J. F. Keffer and W. D. Baines, The round turbulent jets in cross flow, *J. Fluid Mech.* **15**, 481–496 (1963).
7. J. F. Keffer, The physical nature of the subsonic jet in a cross-stream, Analysis of a Jet in a Subsonic Crosswind, NASA Technical Notes, SP-218, pp. 19–36 (1969).
8. J. L. Platten and J. F. Keffer, Deflected turbulent jet flows, *J. Appl. Mech.* **38**, 756–758 (1971).
9. Z. M. Moussa, J. W. Trischka and S. Eskinazi, The near field in the mixing of a round jet with a cross stream, *J. Fluid Mech.* **80**, 49–80 (1977).
10. M. A. Patrick, Experimental investigation of the mixing and penetration of a round turbulent jet injected perpendicularly into a traverse stream, *Trans. Instn Chem. Engrs* **45**, 16–31 (1967).
11. G. Gelb and W. Martin, An experimental investigation of the flow field about a subsonic jet exhausting into a quiescent and a low velocity air stream, *Can. Aero. Space J.* **12**, 333–342 (1966).
12. J. C. Wu, H. M. McMahon, D. K. Mosher and M. A. Wright, Experimental and analytical investigations of jets exhausting into a deflecting stream, *J. Aircraft* **7**, 44–51 (1970).
13. H. M. McMahon and D. K. Mosher, Experimental investigation of pressures induced on a flat plate by a jet issuing into a subsonic crosswind, Analysis of a Jet in a Subsonic Crosswind, NASA SP-218, pp. 49–62 (1969).

14. R. J. Margason, Jet-wake characteristics and their induced aerodynamic effects on V/STOL aircraft in transition flight, NASA SP-218, pp. 1–18 (1969).
15. H. M. McMahon, D. D. Hester and J. G. Palfery, Vortex shedding from a turbulent jet in a crosswind, *J. Fluid Mech.* **48,** 73–80 (1971).
16. W. T. Mikolowsky and H. M. McMahon, An experimental investigation of a jet issuing from wing in a cross flow, *J. Aircraft* **10,** 546–553 (1973).
17. J. W. Ramsey, The interaction of a heated air jet with a deflecting flow, Ph.D. Thesis, University of Minnesota, Minneapolis, Minnesota (1969).
18. J. W. Ramsey and R. J. Goldstein, Interaction of a heated jet with a deflecting stream, *J. Heat Transfer* **93,** 365–372 (1971).
19. J. F. Campbell and J. A. Schetz, Penetration and mixing of heated jets in a waterway with applications to the thermal pollution problem, AIAA paper No. 71-524 (1971).
20. Y. Kamotani and I. Greber, Experiments on turbulent jet in a cross flow, *AIAA J.* **10,** 1425–1429 (1972).
21. G. Rudinger, Experimental investigation of gas injection through a transverse slot into a subsonic cross flow, *AIAA J.* **12,** 566–568 (1974).
22. P. Chassing, J. George, A. Claria and F. Sananes, Physical characteristics of subsonic jets in a cross stream, *J. Fluids Mech.* **62,** 41–65 (1974).
23. G. Bergeles, A. D. Gosman and B. E. Launder, The near field character of a jet discharged normal to a main stream, *J. Heat Transfer* **98,** 373–378 (1976).
24. D. Crabb, D. F. G. Durao and J. H. Whitelaw, A round jet normal to a cross flow, *J. Fluids Engng* **103,** 142–153 (1981).
25. N. Rajaratnam and T. Gangadharaiah, Entrainment by circular jets in cross flow, *J. Wind Engng Ind. Aerodynamics* **9,** 251–255 (1982).
26. J. Andrepoulos, Measurements in a pipe flow issuing perpendicularly into a cross stream, *J. Fluids Engng* **104,** 493–499 (1982).
27. J. Andrepoulos, Heat transfer measurements in a heated jet-pipe flow issuing into a cold cross-stream, *Phys. Fluids* **26,** 3201–3210 (1983).
28. J. Andrepoulos, On the structure of jets in a cross flow, *J. Fluid Mech.* **157,** 163–197 (1985).
29. S. A. Sherif and R. H. Pletcher, Measurements of the flow and turbulence characteristics of round jets in cross flow, *J. Fluids Engng* **111,** 165–171 (1989).
30. S. A. Sherif and R. H. Pletcher, Measurements of the thermal characteristics of heated turbulent jets in cross flow, *J. Heat Transfer* **111,** 897–903 (1989).
31. S. A. Sherif and R. H. Pletcher, Jet-wake thermal characteristics of heated turbulent in cross flow, *J. Thermophys. Heat Transfer* **5,** 181–191 (1991).
32. J. L. Platten and J. F. Keffer, Entrainment in deflected axisymmetric jets at various angles to the stream, Mechanical Engineering Rept. TP-6808, University of Toronto, Ontario, Canada (1968).
33. H. Ziegler and P. T. Wooler, Multiple jets exhausting into a cross flow, *J. Aircraft* **8,** 414–420 (1971).
34. J. H. Kim, An analytical model for the buoyant jet injected into pipe flow, *J. Heat Transfer* **107,** 630–635 (1985).
35. A. R. Karagozian, An analytical model for the vorticity associated with a transverse jet, *AIAA J.* **24,** 429–436 (1986).
36. J. C. Chien and J. A. Schetz, Numerical solution of three-dimensional Navier–Stokes equations with applications to channel flows and a buoyant jet in a cross flow, *J. Appl. Mech.* **42,** 575–579 (1975).
37. S. V. Patankar, D. K. Basu and S. A. Alpay, Prediction of the 3-dimensional velocity field of a turbulent deflected jet, *J. Fluids Engng* **99,** 758–762 (1977).
38. G. Bergeles, A. D. Gosman and B. E. Launder, The turbulent jet in a cross stream at low injection rates: a three-dimensional numerical treatment, *Numer. Heat Transfer* **1,** 217–242 (1978).
39. A. O. Demuren, Numerical calculations of steady 3-dimensional turbulent jets in cross flow, *Comput. Meth. Appl. Mech. Engng* **37,** 309–328 (1982).
40. F. Lana and P. L. Viollet, Three dimensional computations of the mixing of a plasma jet in a cold flow, *Proceedings of ISPC-8*, Tokyo, Vol. 1, pp. 31–36 (1987).
41. M. I. Boulos, J. T. Mostaghimi and P. Proulx, High frequency induction plasma: HiFi computer code, Chemical Engineering Department, University of Sherbrooke, Québec, Canada (1989).
42. R. Bird, W. E. Stewart and E. N. Lightfoot, *Transport Phenomena*, p. 780. Wiley, New York (1960).
43. S. V. Patankar and D. B. Spalding, A calculation procedure for heat, mass and momentum transfer in parabolic flows, *Int. J. Heat Mass Transfer* **15,** 1787–1806 (1971).
44. S. V. Patankar, *Numerical Heat Transfer and Fluid Flow*, p. 197. McGraw-Hill, New York (1980).